# AIR EXCHANGE MEASUREMENTS IN A HIGH-RISE OFFICE BUILDING

by

C. M. Hunt and S. J. Treado

## ABSTRACT

Air exchange rates were measured in the tower of an 11-story office building using $SF_6$ as a tracer gas. Inside-outside pressure difference measurements were also monitored as a function of temperature and wind speed. Fall and winter air exchange rates, I ($hr^{-1}$), measured with make-up and main exhaust pathways blocked could be represented as a function of wind speed, W (mi/hr), by the equation

$$I = 1.08 + 0.036W - 0.0005W^2, \quad \sigma = 0.15.$$

Wind direction, and temperature difference (stack effect), exerted little effect on air exchange rate. In this building, toilet exhausts and other weather independent mechanisms were more important than natural infiltration in producing air exchange. Also, a preliminary analysis of predicted air infiltration by the Shaw-Tamura model was undertaken. The results of this preliminary analysis were consistent with the observations that the stack effect was unimportant and that natural infiltration contributed only part of the total air exchange. However, the plot of calculated infiltration rate as a function of wind speed, using the Shaw-Tamura model, had a different form from the plot of measured data.

Key words: Building air exchange; commercial building ventilation; energy consumption by buildings; office building ventilation; ventilation analysis; weather and building air exchange

## INTRODUCTION

It has been estimated that the operation of commercial buildings in the United States uses approximately 5.5 million barrels of oil a day [1]. Office buildings as well as other buildings with central heating and cooling and forced-air ventilation comprise a major segment of this building stock. Air exchange is an important component of energy usage. However, in the development of conservation measures and the design of new buildings, less is known about the losses due to air infiltration and other mechanisms of air exchange in large buildings than in in single-family residences.

It is fair to say that large office buildings differ from single-family residences not merely in scale but in the complexity of their ventilating systems, which are custom designed for each building. A home may have a single ventilation system or none at all; a large building may have several, each serving a different zone. A home usually depends on infiltration for ventilation; a large building has both infiltration and forced-air intakes and exhausts. The air exchange rate of a large office building is the result of a composite effect of wind, inside-outside temperature difference and the building ventilation system. The present study attempts to measure and interpret the effects of these components.

The most extensive analyses of air exchange in high-rise buildings to date are those of Tamura and others at the National Research Council of Canada [2-10]. Jackman [11], and Barrett and Locklin [12] have also contributed analyses of this subject. Cockroft [13] and deGids [14] have developed analyses of flows and air exchanges in buildings, but these latter analyses were not primarily oriented toward tall buildings. The paper by Shaw and Tamura [9] is of particular interest, because it develops a comparatively simple computational scheme for calculating infiltration rates of tall buildings. However, it is based on wind tunnel measurements of models and determination of the average flow resistance of the

building envelope by pressurization measurements. It has been compared with tracer gas measurements of infiltration rates of houses [15] but not for large buildings. Tracer gas measurements of large buildings have been made [17-19], but attempts to correlate them with computational models are at an early stage.

This paper reports experimental measurements of the ventilation of an eleven story office building by tracer gas techniques and correlation of the results with concurrent weather data and inside-outside pressure difference measurements. The ultimate purpose of such measurements is to be able to test computational models of air exchange in large buildings, such as the model of Shaw and Tamura [9], and to aid the development of improved models. This study is also a test of measurement methodology.

## DESCRIPTION OF BUILDING AND ITS VENTILATION SYSTEM

The measurements described in this paper were made in the Administration Building of the National Bureau of Standards. It is an eleven-story office building surrounded by low lying buildings and open space. A view of the building is shown in Figure 1. A schematic representation of the main features of the building and its ventilation system is shown in Figure 2. Floors two through eleven, referred to as the tower, were the primary focus of this study. These are served by four air handling units located in the mechanical equipment room which occupies the mezzanine between the first and second floors. These units are designated as 3, 4, 5 and 6. All four of the units supply air to part of each floor of the tower as shown in the schematic diagram in Figure 3. Unit 3 serves the west end of each floor, unit 6 the east, while 4 and 5 serve the north and south sides, respectively. Return air from floors 7 through 11 comes back air handling units

3 and 4, while return air from the rest of the tower goes to units 5 and 6. Thus the ventilation system provides for distribution and mixing of air throughout the tower.

The main air supplies to the tower are summarized in Table 1. These estimates were based on anemometer scans of the downstream faces of the filters. They indicate a total volume of air moved within the building equivalent to 4.5 air changes per hour ($hr^{-1}$). A typical estimate of outside make-up air was approximately 0.3 $hr^{-1}$. However, make-up air dampers can modulate the rate of air intake. To eliminate the possibilty of variation of make-up air and to permit operation with recirculated air, special frames covered with sheets of polyethylene were installed in each air handling unit. A door was built into each frame which could be opened to permit normal operation of the system or closed to block makeup air. The exhaust of each air handling unit was also blocked during air exchange measurements. The points of blockage are shown in Figure 3. Except where otherwise stated all measurements were made with make-up and exhaust vents of each air handling unit blocked.

In addition to the main air flows indicated in Table 1, toilets and elevators were vented to the roof. There were also exchanges with the mechanical equipment room through the small grille in the return loop shown as S in Figure 3. This grille is present in three of the four units. When the make-up and exhaust vents were blocked, the grilles of two of the units acted as intakes, because the supply fan delivered more air than the return fan. Toilet, elevator and mechanical equipment room air exchange rates are summarized in Table 2. Air was diverted to the first floor from units 3 and 4 and this too is listed in the table. The effect of the foregoing flows, as well as exchanges with other parts of the building and losses through the stairwell exhausts (which were turned off), have

not been independently quantified, but they are assumed to provide a nearly constant component of the air exchange rate in addition to infiltration.

Besides the mechanical system the dimensions of the building provide important parameters of the ventilation system. The base dimensions of the tower are 220 ft x 44 ft (67 x 13m) and the height, excluding the penthouse, is 102 ft. (31 m). This corresponds to a gross volume of 990,000 $ft^3$ (28,000 $m^3$). Allowing fifteen per cent of the volume for inside walls, partitions and furnishings results in an estimated net volume of 840,000 $ft^3$ (24,000 $m^3$). This estimate has been used used for converting volume flow rates to air changes per hour and vice versa. The envelope area of the tower, including top and bottom surfaces, is estimated to be 73,000 $ft^2$ (7,200 $m^2$).

## EQUIPMENT AND METHODS

Sulfur hexafluoride ($SF_6$) tracer gas concentrations were measured with a small chromatograph equipped with an electron capture detector, an internal sampling pump and rotary sampling valve. A timer-controlled system of valves and an auxiliary pump were used to draw air to the chromatograph probe from different parts of the building in timed sequence. This sampling system is a compact modification of one previously described [20, 21].

Tracer gas was simultaneously fed into the return fans of the four air handling units through four polyethylene tubes of equal length diverging from a floor divider. A similar system was used to sample air. After introduction of tracer gas, and allowing several minutes for the ventilating system to distribute it throughout the building, samples were taken at eight-minute intervals and analyzed for $SF_6$. When the tracer gas decay rate stabilized, air exchange rate was determined from the slope of the decay plot according to the equation

$$I = \frac{-1}{t} \ln \frac{c}{c_o} \qquad (1)$$

where

$I$ = air exchange rate in air changes per hour ($hr^{-1}$)

$c$ = tracer concentration after elapsed time $t$

$c_o$ = initial tracer concentration at arbitrarily selected time $t = t_o$

$t$ = elapsed time in hours.

In special tests, average air exchange rates obtained by separately analyzing the individual air handling units agreed within 0.01 $hr^{-1}$ with the value obtained from the composite samples from the flow divider. A similar average based on twelve sample series taken at local sites of different floor levels throughout the building agreed within 0.05 $hr^{-1}$ with average of the composite samples although individual deviations as large as 0.4 $hr^{-1}$ were observed. Also tracer gas decay rates at the local sites required ten to fifteen minutes longer to stabilize than those obtained from the air handling units.

Inside temperature measurements were made with a thermocouple mounted in return of Air Handling Unit 6. This was supplemented by thermometer measurements in the halls and stairwells at the second and eleventh floor levels on occasions when the main fans were off. Outside temperature measurements were made with a shielded thermocouple located on the north side of the building at the level of the mechanical equipment room between the first and second floor.

Inside-outside pressure measurements were made on the north side of the building with probes at the second and eleventh story levels as indicated in Figure 2. Pressures were transmitted to a variable capacitance gauge through 1/4 in. (6 mm) i.d. polyethylene tubing similar to that used in tracer gas measurements. Outside probes were shielded with 3-liter cylindrical enclosures with several perforations. These were designed to damp velocity pressure.

Wind speed and direction were measured by a sensor 12 ft (3.7 m) above the north face of the penthouse. Off-site wind measurements were obtained from National Climatic Center data taken at National Airport, located about twenty-two miles (35km) southeast of the National Bureau of Standards site. All correlations are based on data from the north sensor.

## TRACER GAS MEASUREMENTS

Air exchange rates with intakes and exhausts of the four air handling units blocked were measured under a range of wind and temperature conditions. The results are shown in Figure 4 where air exchange rate is plotted against inside-outside temperature difference. The figure is subdivided into a number of fields in order to examine different wind-speed ranges separately. It was found that air exchange rate showed very little temperature dependence even at low wind speeds when the effect would be expected to be greatest. Obviously there should be significant stack pressures in a building of this height, so this behavior needs some explanation.

It has been well-established in single-family residences that above certain wind speeds infiltration rate is wind dominated [22, 23, 24]. The modeling analysis of a tall building by Jackman [11] predicted that the combined effect of wind and stack effect at 10 and 20 mi/hr would have been scarcely different than the effect of wind alone. Also the analysis of Sinden [24] shows that the combined effect of wind and stack effect should be subadditive. Likewise the "box" experiments of Blomsterberg and Harrje [26] have demonstrated mechanisms whereby the wind pressures and stack pressures can either interfere with or reinforce each other, depending upon location of the openings. In an exposed building wind effects would be maximized.

The ratio of the lateral surface area to the cross-sectional area of the building was about 5.5 to 1. As building height increases, lateral surfaces over which stack pressures must compete with wind pressures are increased, while internal vertical pathways are proportionally smaller than in single-family residences. In the Administration Building stairwells and elevator shafts comprise less than six percent of the cross-sectional area, and these are accessible only through normally closed doors. According to Jackman's analysis [11] stairwell doors should reduce air infiltration due to stack effect. Thus there are a number of factors which may contribute to weak temperature dependence.

Treating the data as a function of wind velocity alone, a least squares plot of the form shown in Figure 5 is obtained. A curve corresponding to a three-parameter model provides the best fit over the range of data collected. This curve levels off with increasing wind speed. These measurements were made between early October 1978 and February 1979 and thus include fall and winter data. Wind direction has also been disregarded in obtaining the best fit in Figure 5. Average deviations from best fit according to wind direction were

| | |
|---|---|
| North | + 0.03 $hr^{-1}$ |
| South | - 0.04 |
| East | - 0.08 |
| West | + 0.04 |

These are less than the normal scatter of data about the regression line. Wind tunnel measurements have demonstrated pressure differences over the surfaces of scale models of tall buildings [9, 10], and similar differences have been measured with actual buildings [27]. However the data obtained here suggest that the linkage between wind direction and air exchange rate is weak. Others have noted this in measurements of single-family residences [28, 30].

The effect of occupancy on average air exchange rate was negligible, but there was some evidence that closed office doors on weekends impeded the distribution of tracer gas.

## INSIDE-OUTSIDE PRESSURE DIFFERENCES

After observing the effect of wind and temperature difference on air exchange rate it is of interest to note their effect on inside-outside pressure difference. The pressure response is made up of an average inside-outside pressure difference plus a fluctuating component. This is illustrated in Figure 6 where tracings of differential pressure vs time at two floor levels and two wind speeds are shown. The pressure difference due to buoyancy of the warmer indoor air (stack effect) is altered by wind, and a pulsed response is also produced. The pulsed response has been previously reported [29, 30].

### Average Pressure Difference and Temperature Difference

Average inside-outside pressure differences was plotted as a function of inside-outside temperature difference in Figure 7. The total pressure difference, $\Delta P_T$, is given by:

where $$\Delta P_T = \Delta P_{11} - \Delta P_2 \qquad (2)$$

$\Delta P_T$ = total pressure difference

$\Delta P_i$ = inside-outside pressure difference at the i-th floor, i=2, 11

$\Delta P_2$ and $\Delta P_{11}$ are usually, but not always, opposite in sign, so that $|\Delta P_T|$ usually larger than $|\Delta P_{11}|$ or $|\Delta P_2|$.

Pressure probes were located on the north side of the building, so Figure 7 includes the responses to wind from the windward, leeward or lateral directions at different times. Wind directions have been divided into ninety degree quadrants, and designated in the figure by identifying symbols.

Referring to Figure 7, the sloped line in each field is an approximation of the total pressure difference due to pure stack effect. At wind speeds of 0-5 mi/hr (0-2.2 m/s) the estimated and measured total inside-outside pressure differences were in approximate agreement. It should be noted here that the net contribution of the main ventilating system to the pressure difference with intakes and exhausts blocked and the toilet exhaust in operation was less than 0.01 mm Hg (1.3 Pa). At higher wind velocities the simple correlation between inside-outside temperature and pressure was lost. This is consistent with the observation that there was no correlation between temperature difference and air exchange rate. However, at wind speeds less than 5 mi/hr (2.2 m/s) presssure difference showed stronger coupling with inside-outside temperature difference than did air exchange rate, possibly because natural infiltration was only part of the total air exchange rate.

Average Pressure Difference and Air Exchange Rate

Fig. 8A shows air exchange rate as a function of $\Delta P_{11}$ and Fig. 8B as a function of $\Delta P_2$. From Fig. 8A it is seen that at the eleventh floor level 1) the average inside pressure was always larger than the outside pressure, 2) the effects of wind direction were lost and 3) the curve levels off at increasing air exchange rates in a somewhat similar manner to Figure 5. At the second floor, as seen in Figure 8B, there were clear directional effects, probably because the probe was more protected from downsweep and lateral air currents due to southerly winds than the probe nearer the top of the building. Due to the location of the sensors on the north side of the building, when the wind blew from the north, inside pressure always registered less than outside pressure. When it blew from the south the opposite was true. When it blew from the west the inside-outside

pressure relationship could shift either way. Thus the wind patterns were different at the two levels, but the difference in air exchange rates were only slightly different regardless of wind direction.

Air flow through a building envelope by fan pressurization or evacuation may may be expressed by the equation

$$Q = kA(\Delta_p)^n \qquad (3)$$

where Q = flow rate

k = flow coefficient

A = area of the building envelope

n = flow exponent

(For this calculation $k = 0.9 \frac{cfm}{ft^2(in\ H_2O)}$ or $1.3 \times 10^{-4} \frac{m^3}{sm^2Pa^{0.65}}$

$A = 73000\ ft^2$ ($7200\ m^2$), $n = 0.65$. The source of these values is given in the section on Equipment and Methods and in the Appendix).

Equation 3 has been converted to air changes per hour and plotted in Figures 8A and B in order to compare projected air exchange rate due to fan pressurization or evacuation, with observed values. It is clear that at low pressure difference measured air exchange rate was much larger than would be predicted from uniform pressurization of the building envelope.

Referring to Table 2, the sum of the various exhaust air flows is sufficient to account for the rather large air exchange rate at low wind speed indicated in Figures 8A and B. However, if this loss were made up through the building envelope there should be a corresponding pressure difference. This difference was not observed, from which it is hypothesized that the loss was made up through unidentified pathways in the mechanical ventilation system rather than by enhanced leakage through the building envelope. The neutral zone of the building lies somewhere below the third floor level which supports this view. A fan system for

pressurizing large buildings is under construction. Perhaps by selectively pressurizing parts of the building it may become possible to identify the leakage paths.

Average Pressure Difference and Wind Speed

In Figure 9A the average inside-outside pressure differences at the second and eleventh floors are plotted as a function of wind speed. Only data obtained with northerly wind was used in this plot, in order to compare it with impact pressure calculated from the equation

$$P_v = 0.000901W^2$$

where $P_v$ = velocity pressure, mm Hg

$W$ = wind speed, mi/hr

(If $P_v$ is in Pascals and W is in m/s, 0.000601 is substituted for 0.000901)

This comparison is of interest, because it is often assumed that the driving pressure in air infiltration is proportional to $W^2$ [4, 14]. According to Figure 9A, this assumption may tend to overestimate the pressure difference, particularly at higher wind speeds. The data also display considerable scatter, perhaps due to superimposed temperature effects, and because wind may vary over a 45° range. Also the effect of turbulence and the action of the fluctuating pressure component on the average pressure difference are not fully understood.

Pressure Difference Fluctuations

The fluctuating component of inside-outside pressure difference increased with wind speed, as shown in Figures 9B and C where the average amplitude of the pressure fluctuations, $\Delta F_2$ and $\Delta F_{11}$, are plotted against wind speed. Equation 4 is included in the plot for comparison. The relationship between $\Delta F$ and wind speed could be better approximated by a straight line than by the equation. It has not been established whether the average pressure difference,

or the fluctuating component or a combination of the two is the primary driving force in infiltration, but according to data presented here neither average nor the fluctuating component varies as $W^2$.

The relationship between air exchange rate and pressure fluctuations is shown in Figure 8C. It is similar in form to Figures 5 and 8A and B where wind speed and average pressure difference were the independent variables.

Grimsrud, Sherman et al. [30, 31] have monitored pressure differences at several points over the surface of a house and found the integrated average pressure difference at each point to be zero. They also developed and tested an air infiltration model using the fluctuating pressure component and obtained good agreement between measured and predicted infiltration rates in many, but not all of the houses they examined. In addition to establishing the importance of pressure fluctuations, their work implied that wind direction was relatively unimportant. Potter [32] measured differential pressures at selected points across the surface of a dwelling unit in an apartment house. He obtained better agreement between infiltration rates measured by tracer gas with those estimated from pressure fluctuations than with infiltration rates calculated from time averaged pressure differences. He also found weak correlation between infiltration rate and wind direction. Thus fluctuating pressure difference as a driving force of infiltration is receiving serious attention at the present time.

## WIND MEASUREMENTS

All wind speed correlations were based on data obtained with a sensor above the north face of the penthouse. Comparing this data for October, November and December with data obtained concurrently at National Airport an average ratio of

on-site to airport wind speed was found to be 0.79, $\sigma = 0.39$. The average wind on-site speed was 11 mi/hr (4.9 m/s). The equation used by Shaw and Tamura [9] for relating weather station data to on-site data is:

$$\frac{V_t}{V_s} = \left[\frac{G_s}{Z_s}\right]^{1/7} \left[\frac{H}{G}\right]^{1/3} \tag{5}$$

where $V_t = W_t$ = Mean wind speed at top of building

$V_s = W_s$ = Mean wind speed at meteorological station

$G_s$ = Gradient height at meteorological station

$Z_s$ = Anemometer height at meteorological station

$H$ = Height of building (top of penthouse)

$G$ = Gradient height at building site.

Both National Airport and the NBS sites are in locations comparatively unobstructed by tall buildings, so a gradient height of 900 ft. (274m) has been used for both $G_s$ and G. $Z_s$ is 65 ft. (20m) and H is 142 ft. (43m) substituting these values in Eq. 5 gives:

$$\frac{V_t}{V_s} = 0.79$$

The close agreement between the measured and calcuated ratio between wind speed at the top of the building and at the airport may be somewhat fortuitous because of the assumptions used to select the gradient height at the two sites and the choice of exponents. However the results suggest that wind speed averaged over the three months would have given acceptable agreement between the two sites using eq. 5, although on our hour-by-hour basis differences might be significant.

Wind direction was in good agreement between the two sites at wind speed greater than 10 mi/hr (4.5 m/s). At slower wind speed the differences were often large.

## SHAW-TAMURA EQUATION

It is difficult to test the Shaw-Tamura relationships, or any infiltration model, with data obtained in this investigation, because a major part of the air exchange was rate due to building exhausts and other mechanisms independent of weather not explicitly identified. Nevertheless, comparison of calculated and experimental results helps define the measurement and computational problems.

Air infiltration rates due to stack effect and wind calculated by the Shaw-Tamura equations are shown as curves A and B in Figure 10. Further details of the calculations are given in the Appendix. The best line fit from Figure 5 was tansposed to Figure 10 as curve C for comparison. Analysis of the combined effect of wind and stack effect indicated that air exchange rate was essentially dominated by wind, and little difference would be observed if the temperature component were ignored. This is at least in qualitative agreement with experimental observations.

If it is assumed that 1.08 $hr^{-1}$ represents the sum of all weather-independent air exchange rates, even though this rate has not been quantitatively accounted for by independent measurement, then any excess over this intercept is treated as the natural infiltration component of air exchange. When the Shaw-Tamura calculation is compared with this segment of the experimental data, the result suggests that the estimated infiltration rates may not be unreasonable. However, aside from the accuracy of the assumptions used in this comparison, the experimentally derived curve levels off while the calculated curve has a continuously increasing slope. The calculated values are lower at low wind speeds and higher at very high wind speeds. The increasing slope is somewhat reminiscent of the impact pressure curve in Figure 9, suggesting that the driving force for flow through the building envelope may not be proportional to wind velocity squared. A somewhat similar effect is shown in comparisons of measured and calculated

data for two houses described by Tamura [15]. However, this point needs further consideration. Flow data of Cockroft and Robertson [33] for air exchange rate when air is directed against a single opening in a chamber has a form at least qualitatively similar to the continuously increasing shape expected from increasing impact pressure. In addition, mobile home data by Goldschmidt et al. [34] shows a dependency of infiltration rate on wind speed which is qualitatively similar to curve B in Figure 10.

## SUMMARY AND CONCLUSIONS

Air exchange rates were measured in the tower of an eleven-story office building using $SF_6$ as a tracer gas. Wind data as well as inside-outside temperature and pressure measurements were also obtained. The results lead to the following conclusions:

1. Fall and winter air exchange rates, I, measured with the makeup and main exhaust pathways blocked could be represented by the regression equation:

$$I = 1.08 + 0.036W - 0.0005W^2, \quad \sigma = 0.15$$

where w = wind speed, $hr^{-1}$

$\sigma$ = Standard deviation $hr^{-1}$

2. Correlation of air exchange rate with wind direction was weak.
3. Correlation of air exchange rate with inside-outside temperature difference was marginal at wind speed below 5 mi/hr (2.2 m/s) and virtually nonexistent at higher wind speeds.
4. The large intercept at zero wind speed is attributed in part to toilet exhausts and air diverted to other parts of the building. The weather independent components of air exchange rate were not quantitatively accounted for.
5. Inside-outside pressure differences displayed an average difference plus a fluctuating component as previously noted by others.

6. Average inside-outside pressure difference was in essential agreement with theoretical stack pressure at wind speed less than 5 mi/hr (2.2 m/s), but at higher wind speed the correlation was lost. This provides a plausible explanation of why air exchange rate showed little or no variation attributable to stack effect.
7. Weather independent air exchange rate greatly exceeded natural infiltration as calculated by the Shaw-Tamura model.
8. Measured air exchange rate as a function of wind speed began to level off at higher wind speed while the model calls for an accelerating air exchange rate with increasing wind speed.

## Acknowledgments

The authors gratefully acknowledge the support of the Department of Energy, Division of Buildings and Systems and particularly Mr. Howard Ross for bringing into focus some of the areas in which the understanding of energy losses in heating and cooling buildings is weak or lacking. The authors are also indebted to Mr. J. N. Brewer, Chief of the Plant Division of the National Bureau of Standards and to members of the Plant Division staff, especially Mr. Daniel Tucker and Mr. Hugh Virts, for permission to complicate their responsibility for maintaining the operation of the building. They further wish to thank Dr. John Orban of the NBS Statistical Engineering Division for performing the statistical analysis of the air exchange rate weather data in Figure 5. Finally, they are grateful for the technical assistance of Messrs. Marc LeMay, John Bean, and Julius Cohen.

REFERENCES


1. Energy Conservation Guidelines for Office Buildings. Study prepared for General Services Administration, Public Buildings Service, by Dubin-Mindell-Bloome Associates in cooperation with the AIA Research Corp. and Heery and Heery, Architects (January 1974).

2. Tamura, G. T., and Wilson, A. G., Pressure Differences for a Nine-Story Building as a Result of Chimney Effect and Ventilation System Operation, ASHRAE Trans. 73 (2) 180-189 (1966).

3. Tamura, G. T., and Wilson, A. G., Pressure Differences Caused by Chimney Effect in Three High Buildings, ASHRAE Trans. 73 (2) 1.1-1.10 (1967).

4. Tamura, G. T., and Wilson, A. G., Building Pressures Caused by Chimney Action and Mechanical Ventilaton, ASHRAE Trans. 73 (2) 2.1-2.12 (1967)

5. Tamura, G. T., and Wilson, A. G., Pressure Differences Caused by Wind on Two Tall Buildings, ASHRAE Trans. 74 (2), 170-180 (1968).

6. Shaw, C. Y., Sander, D. M., and Tamura, G. T., Air Leakage Measurements of the Exterior Walls of Tall Buildings, ASHRAE Trans. 79 (2) 40-48 (1973).

7. Sander, D. M., and Tamura, G. T., Simulation of Air Movement in Multi-Story Buildings. Paper presented at Second Symposium on the Use of Computers for Environmental Engineering Related to Buildings, Paris, June 13-15 (1974).

8. Tamura, G. T., Shaw, C. Y., Studies on Exterior Wall Air Tightness and Air Infiltration of Tall buildings, ASHRAE Trans. 82 (1) 122-133 (1976).

9. Shaw, C. Y., and Tamura, G. T., The Calculation of Air Infiltration Rates Caused by Wind and Stack Action for Tall Buildings, ASHRAE Trans. 83 (2), 145-158 (1977).

10. Shaw, C. Y., A Method for Predicting Air Infiltration Rates for a Tall Building Surrounded by Structures of Uniform Height, ASHRAE Trans. 85 (1), 72-84 (1979).

11. Jackman, P. J., A Study of the Natural Ventilation of Tall Office Buildings, J. Inst. Heating and Ventilating Eng. 38, 103-118 (1970).

12. Barrett, R. E., and Locklin, D. W., Computer Analysis of Stack Effect in High-Rise Buildings, ASHRAE Trans. 74 (2) 155-169 (1968).

13. Cockroft, J. P., Air Flows in Buildings, Inst. of Mathematics and Its Applications, Symposium on The Environment Inside Buildings, London, 2 May (1979).

14. deGids, W. F., Calculation Method for the Natural Ventilation of Buildings, Seventh TNO/TVVL Seminar, October 1977. Publication 633 of the TNO Res. Inst. for Environmental Hygiene, P. O. Box 214, Delft, The Netherlands.

15. Tamura, G. T., The Calculation of House Infiltration Rates, ASHRAE Trans. 85 (1), 58-71 (1979).

16. Ross, H., and Grimsrud, D., Air Infiltration in Buildings: Literature Survey and Proposed Research Agency, LBL-W7822, UC-95d. Report prepared for International Energy Agency, U. S. Department of Energy (May 1978).

17. Kelnhofer, W. J., Hunt, C. M., and Didion, D. A., Determination of Combined Air Exfiltration Rates in a Nine-Story Office Building, Proc. of the Conf. on Improving Efficiency and Performance of HVAC Equipment and Systems for Commercial and Industrial Buildings, Vol. II, Purdue University, April 12-14 (1976).

18. Hunt, C. M., Ventilation Measurements in the Norris Cotton Federal Office Building in Manchester, N.H., ASHRAE Trans. 85 (1) 828-839 (1979).

19. Harrje, D. T., and Cooper, J. B. (with special assistance from Thomas A. Mills, Jr.), Instrumenting Energy Audits, Princeton University Center for Energy and Environmental Studies, Report No. 91 (July 1979).

20. Harrje, D. T., Hunt, C. M., Treado, S., and Malik, N., Automated Instrumentation for Building Infiltration Measurements, Princeton University Center for Environmental Studies Report No. 13 (1975).

21. Hunt, C. M., and Treado, S., A Prototype Semi-Automated System for Measuring Air Infiltration in Buildings Using Sulfur Hexafluoride as a Tracer, National Bureau of Standards Technical Note 898 (March 1976). The essential features of this system are also described in reference 20.

22. Dick, J. B., and Thomas, D. A., Ventilation Research in Occupied Houses, J. Instit. of Heating and Ventilating Eng. 19 306-326 (1951).

23. Mattingly, G.E., Harrje, D.T., Heisler, G.M. The Effectiveness of an Evergreen Windbreak for Reducing Residential Energy Consumption, ASHRAE TRANS. 85 (2) (1979.

24 Malik, N. Air Infiltration in Homes; M. S. Thesis in Engineering, Princeton Univ. Center for Environmental Studies Report PU/CES 58 (1977).

25. Sinden, F. G., Wind, Temperature and Natural Ventilation -- Theoretical Considerations, Energy and Buildings 1, 275-280 (1977/78).

26. Blomsterberg, A. K., and Harrje, D. J., Approaches to the Energy Losses in Buildings, ASHRAE Trans. 85 (1) 797-814 (1979).

27. Ham, Ph.J., Comparison of Internal and Outside Pressure Distributions Measured at a Model and at the Actual Slatervaart Hospital in Amsterdam, Seventh TNO/TVVL Seminar, Oct. 1977. Publ. 629 of the TNO Res. Institute for Environmental Ygience, P. O. Box 214, Delft, The Netherlands.

28. Sepsy, C. F., Jones, C. D., McBride, M., and Blancett, R., EPRI Final Report, Ohio State University, Environmental Control Group, Dept. of Mech. Engrg., Columbus, O, Chapter 9 -- Air Infiltration.

29. Hill, J. E. , and Kusuda, T., Dynamic Characteristics of Air Infiltration, ASHRAE Trans. 81 (1), 168-185 (1975).

30. Grimsrud, M. H., Sherman, M. C., Diamond, R. C., and Condon, P. E., Infiltration-Pressurization Correlations: Detailed Measurements on a California House, ASHRAE Trans. 85 (1) 851-864 (1979).

31. Sherman, M. H., Grimsrud, D. T., and Diamond, R. C., Infiltration-Pressurization Correlations: Surface Pressures and Terraine Effects, ASHRAE Symposium Paper DE-79-1, No. 4, Detroit (June 1979).

32. Potter, I. N., Effect of Fluctuating Wind Pressures on Natural Ventilation Rates, ASHRAE Symposium Paper DE-79-1, No. 3, Detroit (June 1979).

33. Cockroft, J. P., an Robertson, P., Ventilation of an Enclosure Through a Single Opening, Building And Environment 11 21-35 (1976).

34. Goldschmidt, V. W., and Wilhelm, D. R., Summertime Infiltration Rates in Mobile Homes, ASHRAE Trans. 85 (1) 840-849 (1979).

## APPENDIX

The Shaw-Tamura equation for relating infiltration rate to wind speed and direction may be expressed in the form

$$Q_w = 6.80 \times 10^{-3}\, C_w L H \alpha V_t^{1.3} \qquad \text{(A-1)}$$

where

$Q_w$ = flow rate at which air enters and leaves the building, cfm

$C_w$ = average flow coefficient of building envelope = 0.9 $\dfrac{\text{cfm}}{\text{ft}^2 \cdot (\text{in } H_2O)^{0.65}}$

L = length of long side of building = 220 ft

H = height of building = 102 ft

$V_t$ = wind speed at top of building

$$\alpha = \frac{Q_w \text{ at wind angle } \theta}{Q_w \text{ at wind angle } 0}$$

$V_t = W$ = wind speed at top of building, mi/hr

(If SI units are used, 0.699 is substituted for $6.80 \times 10^{-3}$, and $C_w = 1.3 \times 10^{-4} \dfrac{m^3}{s \cdot m^2 Pa^{0.65}}$.)

The average flow coefficient $C_w$ was obtained by measuring the increase in pressure when make-up air was admitted to the building. An increase in flow of 4600 cfm resulted in an increase in pressure of 0.031 mm Hg. This was a low value and could only be measured on a calm day. Also a single point does not permit experimental determination of the flow exponent, so 0.65 is used. Nevertheless, these measurements permit approximations to be made and also allow some general observations regarding application of Equation A-1.

The direction coefficient $\alpha$ was assumed to be unity. This is equivalent to treating the data as if the wind were always blowing normally against the broad side of the building. As noted in the text, linkage between wind direction and air change rate was weak. Finally, onsite rather than airport wind data were used.

The equation for calculating the stack effect has the form

$$Q_s = C_w S \quad 0.52\gamma P \left[\frac{\Delta T}{T_i T_o}\right]^n \left[\frac{\beta H}{n+1}\right]^n \qquad \text{(A-2)}$$

where

$Q_s$ = flow rate at which air enters and leaves the building due to stack effect

$S$ = building perimeter, 528 ft

$\gamma$ = ratio of actual to theoretical pressure difference = 0.8

$P$ = atmospheric pressure = 14.7 lb/in$^2$

$T_o$ = absolute outside temperature, R

$T_i$ = absolute inside temperature, R

$\Delta T = T_i - T_o$

$n$ = flow exponent = 0.65

$\beta$ = ratio of height of neutral zone to building height = 0.5

Other symbols are defined in connection with equation A-1. (If SI units are used, 0.0342 is substituted for 0.52 in equation A-2.)

The value of $\gamma$=0.8 for an office building was taken from Shaw and Tamura. Comparison of inside-outside pressures with the inside probes in the halls and in the open stairwells suggests that this was a reasonable estimate. The flow exponent 0.65 was also taken from Shaw and Tamura. Exponents between 0.6 and 0.7 are quite typical. A value of $\beta$=0.5 was used. Experimental estimates of

the neutral zone obtained by extrapolating a 2-point plot of $\Delta P_{11}$ vs $\Delta P_2$ vs elevation through the point of zero pressure difference gave an average at 2nd the floor level, but individual estimates ranged from 5th floor to below the basement. Thus, $\beta$=0.5 provides an upper estimate of the effect of air buoyancy on air infiltration rate. It should also be noted that equation A-2 is more sensitive to uncertainties in $\beta$ than uncertainties in $C_w$, but $\beta$ is the more difficult to measure.

The equation for estimating the combined effect of wind and stack action is:

$$\frac{Q_{ws}}{Q_{lrg}} = 1 + 0.24 \left[\frac{Q_{sml}}{Q_{lrg}}\right]^{3.3} \qquad \text{(A-3)}$$

where

$Q_{ws}$ = flow rate caused by combined wind and stack action

$Q_{lrg}$ = larger value of $Q_w$ and $Q_s$

$Q_{sml}$ = smaller value of $Q_w$ and $Q_s$

Table 1

Supply and Minimum Outside Air to Tower

| Unit | Supply air[1/] | | Minimum[2/] outside air | |
|---|---|---|---|---|
| | cfm | $m^3/s$ | cfm | $m^3/s$ |
| 3 | 14,600 | 6.9 | 2,400 | 1.1 |
| 4 | 19,200 | 9.1 | 1,100 | 0.5 |
| 5 | 18,700 | 8.8 | 500 | 0.2 |
| 6 | 13,800 | 6.5 | 400 | 0.2 |
| Total | 66,300 | 31.3 | 4,400 | 2.0 |
| Air changes per hr | 4.7 | | 0.31 | |

1/ Obtained with outside air blocked.

2/ The amount of outside air can vary, but these are representative settings.

Table 2

Summary of Remaining Building Air Exhausts and Exchanges With Main Air Handling Units in Complete Recirculation Mode

| | cfm | $m^3/s$ | $hr^{-1}$ |
|---|---|---|---|
| Toilet exhausts (Fig. 2) | 6,100 | 2.9 | 0.44 |
| Elevator vent (Fig. 2) | 1,500 | 0.7 | 0.11 |
| Air diverted to first floor (Fig. 3) | 10,000[1] | 4.7[1] | 0.72[1] |
| Exchange with mechanical equipment room (Fig. 3) | | | |
| Unit 4 | -2,800[2] | 1.3[2] | -0.20[2] |
| Unit 5 | -1,300[2] | 0.6[2] | -0.09[2] |
| Unit 6 | 890 | 0.4 | 0.06 |

[1]Based on hot-wire anemometer measurement, all others based on vane anemometer measurement.

[2]Negative sign signifies air is drawn into ventilation system.

## Legends to Figures

Figure 1. National Bureau of Standards Administration Building, viewed from southeast.

Figure 2. Schematic representation of the main features of the ventilation system of the NBS Administration Building tower.

Figure 3. Diagram of air movements to and from the four air handling systems of the NBS Administration Building tower.

| | |
|---|---|
| ↶ - Damper | E - Exhaust air |
| FL - Floor | S - Air to mechanical equipment room |
| M - Makeup air | B - Points of added blockage |

Figure 4. Air exchange rate as a function of inside-outside temperature difference. Figure is subdivided into class intervals according to wind speed.

Figure 5. Fall-winter air exchange rate as a function of wind speed.

Figure 6. Pressure difference vs time at high and low wind speeds.
Upper chart, wind 4 mi/hr (1.7 m/s), $\Delta$T 21°C.
Lower chart, wind 33 mi/hr (15 m/s), $\Delta$T 21°C.
Left, $\Delta$p 2nd floor; right, $\Delta$p 11th floor.
Full scale represents -0.5 mm Hg (-67 Pa) to +0.5 mm Hg (+67 Pa).

Figure 7. Average inside-outside pressure difference as a function of inside-outside temperature difference. Figure is subdivided into class intervals according to wind speed.

Figure 8. Air exchange rate as a function of inside-outside pressure difference
A - average pressure difference at 11th floor, $\Delta p_{11}$
B - average pressure difference at 2nd floor, $\Delta p_2$
C - average fluctuating component of pressure difference, $\Delta F_T = \Delta F_2 + \Delta F_{11}$.

Figure 9. Inside-outside pressure difference as a function of wind speed
A - average pressure difference in response to wind from north
B - average fluctuating component of pressure difference at 11th floor, $\Delta F_{11}$
C - average fluctuating component of pressure difference at 2nd floor, $\Delta F_2$.

Figure 10. Comparison of measured average air exchange rate with infiltration rate calculated by Shaw-Tamura equations.
Curve A - calculated infiltration rate due to stack effect

Curve B - calculated infiltration rate due to wind (essentially equal to combined effect of wind and stack action)

Curve $B^1$ - curve B transposed with intercept at 1.08

Curve C - best fit air exchange rate vs wind speed, transposed from Figure 5.

FIG. 1

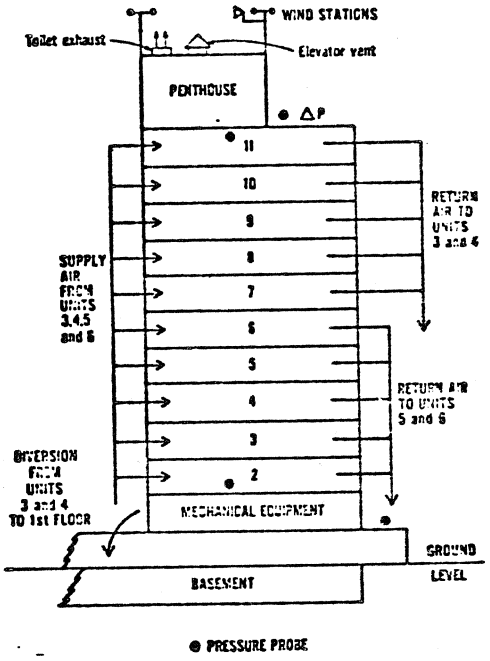
WIND STATIONS
Toilet exhaust
Elevator vent
PENTHOUSE
ΔP
11
10
9
8
7
6
5
4
3
2
RETURN AIR TO UNITS 3 and 4
SUPPLY AIR FROM UNITS 3,4,5 and 6
RETURN AIR TO UNITS 5 and 6
DIVERSION FROM UNITS 3 and 4 TO 1st FLOOR
MECHANICAL EQUIPMENT
GROUND LEVEL
BASEMENT
PRESSURE PROBE

Fig 2

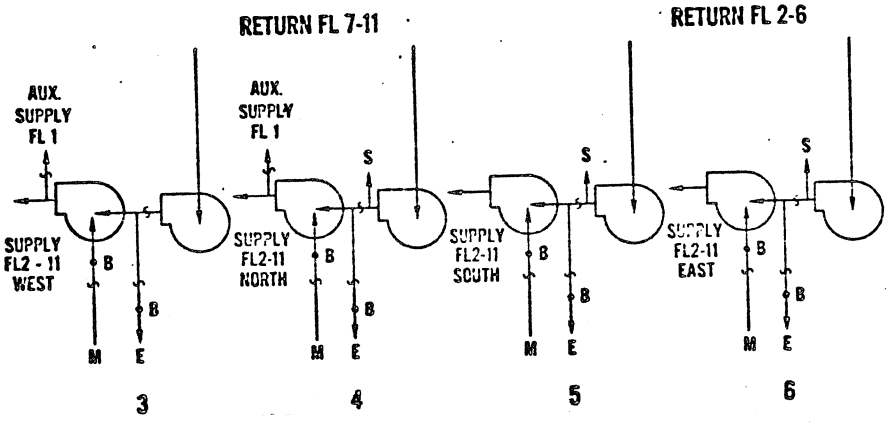
RETURN FL 7-11
RETURN FL 2-6
AUX. SUPPLY FL 1
AUX. SUPPLY FL 1
S
S
S
SUPPLY FL2 - 11 WEST
SUPPLY FL2-11 NORTH
SUPPLY FL2-11 SOUTH
SUPPLY FL2-11 EAST
B
B
B
B
B
B
B
B
M
E
M
E
M
E
M
E
3
4
5
6

FIG 3

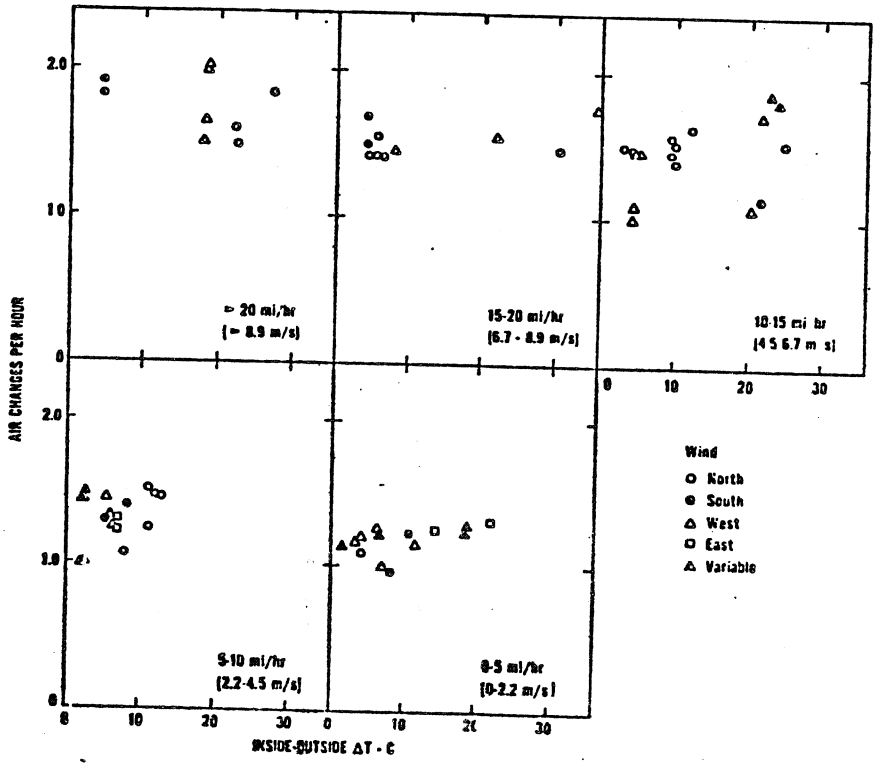
AIR CHANGES PER HOUR
2.0
1.0
0
2.0
1.0
0
> 20 mi/hr
(> 8.9 m/s)
15-20 mi/hr
(6.7 - 8.9 m/s)
10-15 mi hr
(4.5 6.7 m s)
5-10 mi/hr
(2.2-4.5 m/s)
0-5 mi/hr
(0-2.2 m/s)
0
10
20
30
INSIDE-OUTSIDE ΔT - C
Wind
North
South
West
East
Variable

FIG 4

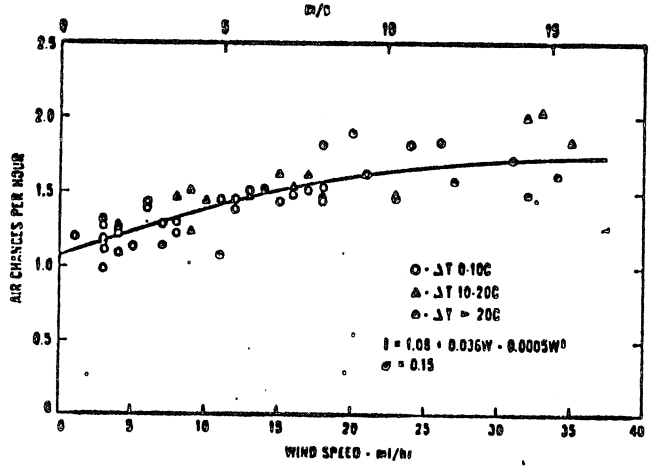
m/s
0
5
10
15
2.5
2.0
1.5
1.0
0.5
0
AIR CHANGES PER HOUR
○ - ΔT 0-10C
△ - ΔT 10-20C
⊖ - ΔT > 20C
I = 1.08 + 0.036W - 0.0005W²
σ = 0.15
0
5
10
15
20
25
30
35
40
WIND SPEED - mi/hr

Fig 5

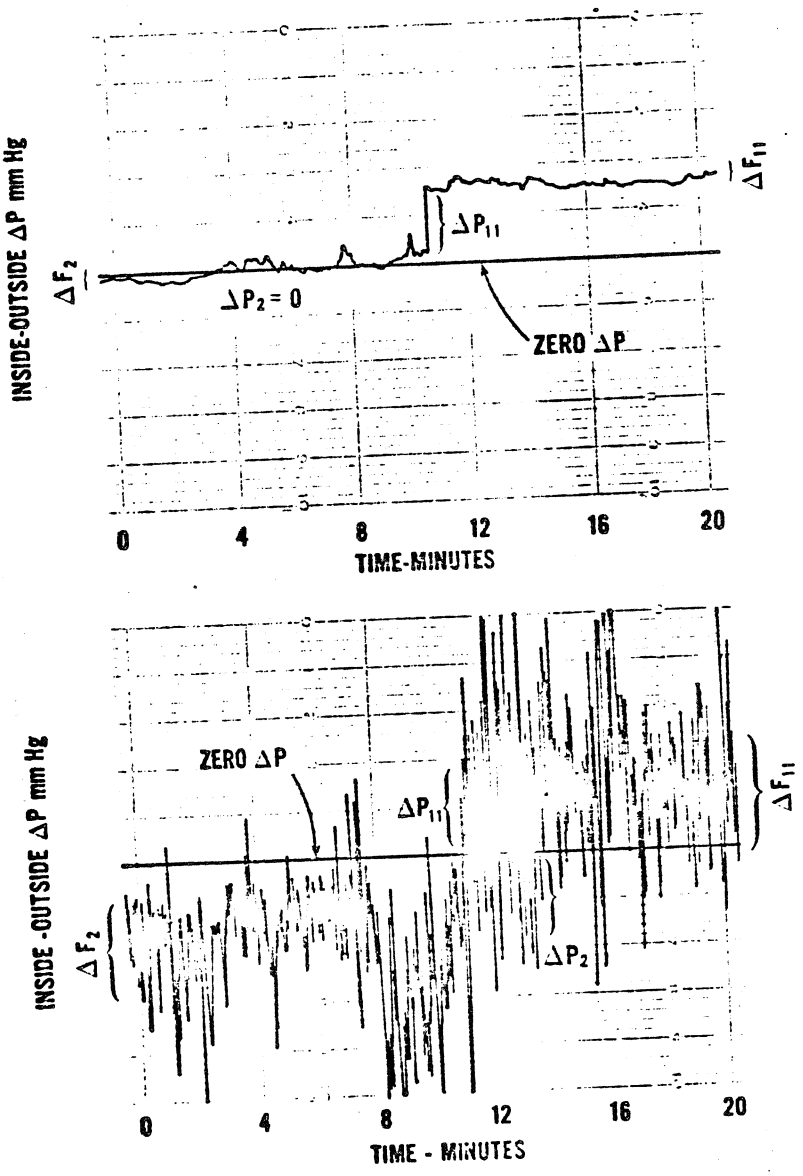
INSIDE-OUTSIDE ΔP mm Hg
ΔF2
ΔP2 = 0
ΔP11
ΔF11
ZERO ΔP
0
4
8
12
16
20
TIME-MINUTES
INSIDE -OUTSIDE ΔP mm Hg
ZERO ΔP
ΔP11
ΔF11
ΔF2
ΔP2
0
4
8
12
16
20
TIME - MINUTES

FIG. 6

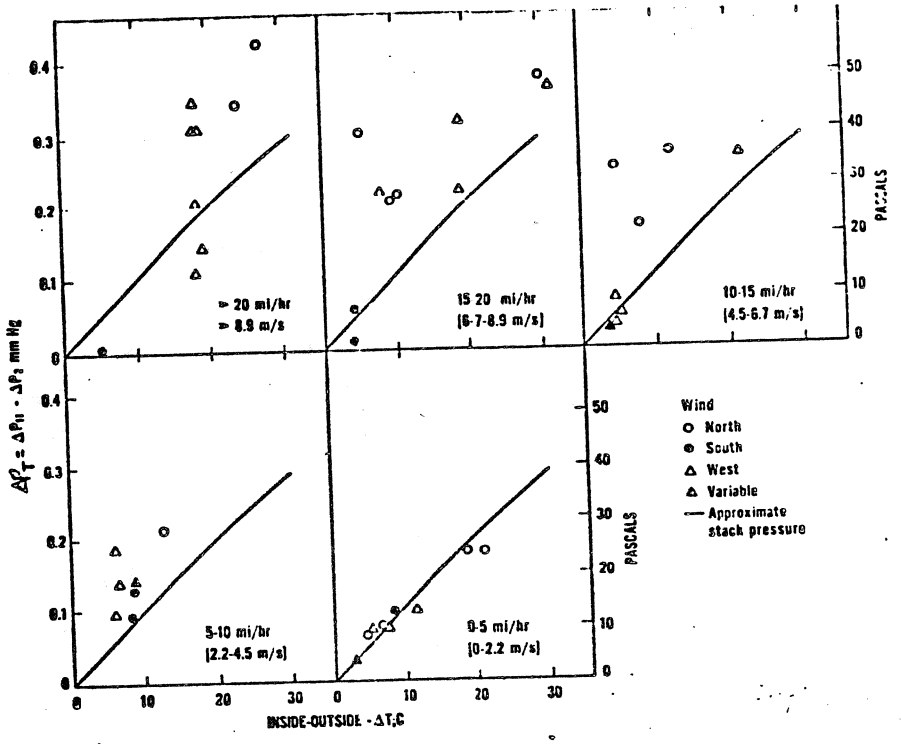
> 20 mi/hr
> 8.9 m/s
15 20 mi/hr
(6-7-8.9 m/s)
10-15 mi/hr
(4.5-6.7 m/s)
5-10 mi/hr
(2.2-4.5 m/s)
0-5 mi/hr
(0-2.2 m/s)
Wind
North
South
West
Variable
Approximate stack pressure
PASCALS
INSIDE-OUTSIDE - ΔT,C

F167

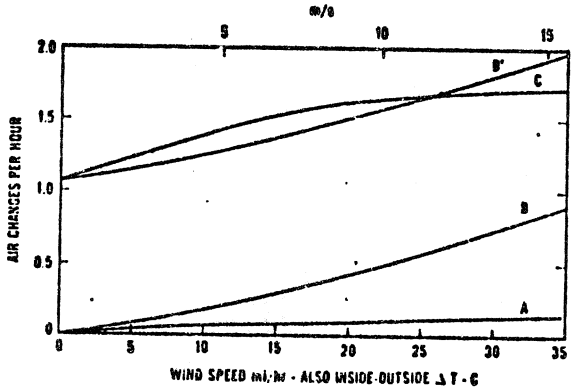
m/s
5
10
15
2.0
1.5
1.0
0.5
0
B'
C
B
A
AIR CHANGES PER HOUR
0
5
10
15
20
25
30
35
WIND SPEED mi/hr - ALSO INSIDE-OUTSIDE Δ T - C

Fig 12